Quadrature Histograms in Maximum Likelihood Quantum State Tomography

J. L. E. Silva,[1] H. M. Vasconcelos,[2,3,*] and S. Glancy[3]

[1] *Departamento de Engenharia de Teleinformática, Universidade Federal do Ceará, Fortaleza, Ceará, 60440, Brazil*

[2] *Departamento de Engenharia de Teleinformática, Universidade Federal do Ceará, Fortaleza, Ceará, Brazil*

[3] *Applied and Computational Mathematics Division, National Institute of Standards and Technology, Boulder, Colorado, 80305, USA*

(Dated: February 7, 2018)

Quantum state tomography (QST) aims to determine the quantum state of a system from measured data and is an essential tool for quantum information. When dealing with quantum states of light, QST is done by measuring quantum noise statistics of the field amplitudes at different optical phases using homodyne detection. The quadrature-phase homodyne measurement outputs a continuous variable, but we can histogram the continuous measurements and make the statistical estimation faster without losing too much information. This paper investigate different ways to determine the quadrature histograms for optical homodyne QST.

PACS numbers: 03.65.Wj, 03.67.-a, 42.50.Dv

I. INTRODUCTION

Quantum information science and engineering is now at the point where rudimentary quantum computers are available in the laboratory and commercially [1–4]. Consequently, precise reconstruction and diagnostic tools used to estimate quantum states [5–12], processes [13–20], and measurements [21–24] are fundamental.

Quantum tomography techniques for quantum states of light became a subject of major interest in recent years, since quantum light sources are essential for implementations of continuous-variable (CV) quantum computation [25–29]. These source are also extensively exploited in quantum criptography [30–34], quantum metrology [35, 36], state teleportation [37–39], dense coding [40, 41] and cloning [42, 43].

In quantum state tomography, we perform a large number of experimental measurements on a collection of quantum systems, all prepared in a same unknown state. The goal is to estimate this unknown state from the experimental measurements results. This estimation can be done from the experimental statistical data by different methods. In here we will be dealing with Maximum Likelihood Estimation (MLE), that finds among all possible states, the one which maximizes the probability of obtaining the experimental data set in hand.

Quantum homodyne tomography is one of the most popular optical tomography techniques available. It rapidly became a versatile tool and has been applied in many different quantum optics experimental settings since it was proposed by Vogel and Risken in 1989 [5] and first implemented by Smithey *et al.* in 1993 [6]. This technique permits to characterize a light quantum state by means of the electric field quantum noise statistics collected through multiple phase-sensitive measurements.

* hilma@ufc.br

A homodyne measurement generates a continuous value. While no data binning is necessarily needed, we believe that the loss due to binning may be insignificant. On the other hand, discretization of the data by binning it reduces considerably the number of data, expediting the reconstruction algorithm. But how can we estimate the quadrature bin width, such that the bins are not too small nor too big? Bins should not be too small in order to guarantee a save in calculation time and memory. And bins should not be too large in order to avoid a lack of resolution, making the histogram a poor representation of the underlying distribution shape.

In this paper, we use numerical experiments to simulate optical homodyne tomography of quantum optical states and perform maximum likelihood tomography on the data with and without binning. When choosing a quadrature bin width, we use and compare two different ways: Scott's rule [44] and equation (5.136) from Leonhardt's book [45]. The paper is divide as follow: in Section II we review maximum likelihood in homodyne tomography. In Section III we describe our numerical experiments and present our results. In Section VI we discuss the interpretation of our results and make some concluding remarks.

II. MAXIMUM LIKELIHOOD IN HOMODYNE TOMOGRAPHY

Let us consider N quantum systems, each of them prepared in an optical state described by a density matrix ρ_{true}. In each experimental run, we measure the field quadrature at different phases θ of a local oscillator, i.e. a reference system prepared in a high amplitude coherent state. Each measurement is associated with an observable $\hat{X}_\theta = \hat{X}\cos\theta + \hat{P}\sin\theta$, where $\hat{X}$ and $\hat{P}$ are the position and momentum operators, respectively. For a given phase θ, we measure a quadrature value x, resulting on

a data set $\{(\theta_i, x_i)\}$.

The outcome of the i-th measurement is described by a positive-operator-valued measure (POVM) element $\Pi(x_i|\theta_i) = \Pi_i$. Given the data set $\{(\theta_i, x_i) : i = 1, ..., N\}$, we can write the likelihood of a candidate density matrix ρ as

$$\mathcal{L}(\rho) = \prod_{i=1}^{N} \mathrm{Tr}(\Pi_i \rho), \tag{1}$$

where $\mathrm{Tr}(\rho\Pi_i)$ is the probability, when measuring with phase θ_i, to obtain outcome x_i, according to the candidate density matrix ρ.

MLE searches within the density matrix space the one that maximizes the likelihood in (1). Equivalently, it usually is more convenient to maximize the logarithm of the likelihood (the "log-likelihood"):

$$L(\rho) = \ln \mathcal{L}(\rho) = \sum_{i=1}^{N} \ln[\mathrm{Tr}(\Pi_i \rho)], \tag{2}$$

which is maximized by the same density matrix as the likelihood. The MLE is essentially a function optimization problem, and since the log-likelihood function is concave, the convergence to an unique solution will be achieved by most iterative optimization methods.

In our numerical simulations, we use an algorithm for likelihood maximization that begins with interactions of the $R\rho R$ algorithm [46] followed by iterations of a regularized gradient ascent algorithm (RGA). The main reason to switch from one algorithm to another is the fact that an expressive slow-down is observed in the $R\rho R$ algorithm after about $(n+1)^2/4$ iterations. In the RGA, $\rho^{(k+1)}$ is parametrized as

$$\rho^{(k+1)} = \frac{\left(\sqrt{\rho^{(k)}} + A\right)\left(\sqrt{\rho^{(k)}} + A^\dagger\right)}{\mathrm{Tr}\left[\left(\sqrt{\rho^{(k)}} + A\right)\left(\sqrt{\rho^{(k)}} + A^\dagger\right)\right]}, \tag{3}$$

where $\rho^{(k)}$ is the density found by the last interaction of $R\rho R$, and A may be any complex matrix of the same dimensions as ρ. Eq. (3) ensures that $\rho^{(k+1)}$ is a physical density matrix for any chosen A. The matrix A should maximize the quadratic approximation of the log-likelihood subject to $\mathrm{Tr}(AA^\dagger) \leq u$, where u is a positive number adjusted by the algorithm to guarantee that the log-likelihood increases with each iteration. To halt the interactions, we use the stopping criterion of [47], $L(\rho_{\mathrm{ML}}) - L(\rho^{(k)}) \leq 0.2$, where $L(\rho_{\mathrm{ML}})$ is the maximum of the log-likelihood.

III. NUMERICAL EXPERIMENTS

Our numerical experiments simulate single mode optical homodyne measurements [48] of Gaussian cat and squeezed vacuum states. Each considered state is represented by a density matrix ρ_{true} in an n photon basis.

In order to calculate the probability to obtain homodyne measurement outcome x, when measuring state ρ_{true} with phase θ, we need to represent $\Pi(x|\theta)$ in the n photon basis considered. If $|x\rangle$ is the photon number basis representation of the x-quadrature eigenstate with eigenvalue x, and $U(\theta)$ is the phase evolution unitary operator, then for an ideal homodyne measurement, we have $\Pi(x|\theta) = U(\theta)^\dagger |x\rangle\langle x| U(\theta)$. Moreover, it is more realistic to consider that homodyne detectors suffer from photon loss, by including that loss in the POVM elements. In this case, the projector operator is replaced by $\Pi(x|\theta) = \sum_{i=1}^{n} E_i(\eta)^\dagger U(\theta)^\dagger |x\rangle\langle x| U(\theta) E_i(\eta)$, where $\eta = 0.9$, which is typical for state-of-the-art homodyne detectors, is used in all simulations. Using this strategy, we are able to estimate the state of the system before the occurrence of the regarded loss. We use rejection sampling from the distribution given by $P(x|\theta)$ to guarantee random samples of homodyne measurement results [49].

To choose the phases at which the homodyne measurements are performed, we divide the upper-half-circle evenly among m phases between 0 and π and measure N/m times at each phase, where N is the total number of measurements. In all simulations, we use $m = 20$ and $N = 20,000$. To secure a single maximum of the likelihood function, we need an informationally complete set of measurement operators, which can be obtained if we use $n+1$ different phases to reconstruct a state that contains at most n photons [45].

To quantify how similar a reconstructed state, ρ, is of a true state, ρ_{true}, we use the fidelity, defined by:

$$F = Tr\sqrt{\rho^{1/2}\,\rho_{\mathrm{true}}\,\rho^{1/2}}. \tag{4}$$

The fidelity shown in the graphs are obtained by calculating the arithmetic mean of the 100 fidelities, since we reconstruct each state 100 times, each time obtaining the fidelity between the reconstructed state and the true state. The uncertainty in each fidelity estimate (shown as error bars in the figures) is the standard deviation of the mean of the fidelity.

We calculate and compare the fidelity between the reconstructed state and the true state for four different situations: (i) the state is reconstructed using the continuous values of homodyne measurement results, that is without binning; (ii) the state is reconstructed using homodyne measurement data binning with a chosen bin width (iii) the state is reconstructed using homodyne measurement data binning with a bin width given by Scott's rule [44]; and (iv) the state is reconstructed using homodyne measurement data binning with a bin width suggested by Leonhardt in [45].

In 1979 Scott derived a formula for the asymptotically optimal bin width:

$$h^\star = \left[\frac{6}{s\int_{-\infty}^{\infty} f'(x)^2 dx}\right]^{1/3}, \tag{5}$$

where $f(x)$ is a continuous probability density function with two continuous bounded derivatives and s is the

sample size. For a Gaussian probability density, we have

$$\int_{-\infty}^{\infty} f'(x)^2 dx = \frac{1}{4\sqrt{\pi}\sigma^3}, \tag{6}$$

where σ is the standard deviation. Combining Eqs. (5) and (6), we obtain the optimal bin width for normal data distribution:

$$h = 3.5\,\sigma\, s^{-1/3}. \tag{7}$$

This formula is known as Scott's rule, and is optimal if the data is close to being normally distributed, but is also appropriate for most other distributions.

On the other hand, Leonhardt states that if we desire to reconstructed a density matrix of a state with n photons, we need a bin width narrower than $q_n/2$, where q_n is given by

$$q_n = \frac{\pi}{\sqrt{2n+1}}. \tag{8}$$

This result was shown initially in [50], and was obtained by using a semiclassical approximation for the amplitude pattern functions in quantum state sampling. This result is also valid for phase-space tomography, since they are both mathematically equivalent. In a real experiment, we probably do not have any knowledge of the quantum state, including the mean number of photons in it. All we have access is to quadrature measurements. To be able to use Eq. (8), we need to find a way to determine the mean photon number from the quadrature measurements. We propose a method to determine the mean photon number from the quadrature measurement results in the next section.

IV. ESTIMATING MEAN PHOTON NUMBER

[SG: Here are some quick and rough notes explaining how we can estimate the mean number of photons. They will need a lot of revision before they are really part of the paper. I am only putting them here, because it seemed like a convenient way to share with Hilma and Leonardo.] In order to use Leonhardt's advice for choosing the histogram bin width, we need to estimate the mean number $\langle n\rangle$ of photons in the measured state from the phase-quadrature data set. To find an estimator, we first compute the mean value of $(\hat{X}_\theta)^2$, averaged over θ, treating θ as if it is random and uniformly distributed between 0 and π.

$$\langle(\hat{X}_\theta)^2\rangle = \langle \hat{X}^2\cos^2\theta + (\hat{X}\hat{P}+\hat{P}\hat{X})\cos\theta\sin\theta + \hat{P}^2\sin^2\theta\rangle \tag{9}$$

The phase θ is independent of $\hat{X}$ and $\hat{P}$, so we can compute the expectation over θ as

$$\langle(\hat{X}_\theta)^2\rangle = \Big\langle \int_0^\pi (\hat{X}^2\cos^2\theta + (\hat{X}\hat{P}+\hat{P}\hat{X})\cos\theta\sin\theta + \hat{P}^2\sin^2\theta)\mathrm{Prob}(\theta)\mathrm{d}\theta\Big\rangle \tag{10}$$

$$\langle(\hat{X}_\theta)^2\rangle = \Big\langle \int_0^\pi (\hat{X}^2\cos^2\theta + (\hat{X}\hat{P}+\hat{P}\hat{X})\cos\theta\sin\theta + \hat{P}^2\sin^2\theta)\frac{1}{\pi}\mathrm{d}\theta\Big\rangle \tag{11}$$

$$= \Big\langle (\hat{X}^2\frac{\pi}{2} + \hat{P}^2\frac{\pi}{2})\frac{1}{\pi}\Big\rangle \tag{12}$$

$$= \frac{1}{2}\left\langle \hat{X}^2 + \hat{P}^2\right\rangle \tag{13}$$

Leonardo showed that

$$\hat{n} = \frac{1}{2}\left(\hat{X}^2 + \hat{P}^2 - 1\right). \tag{14}$$

Therefore

$$\langle\hat{n}\rangle = \frac{1}{2}\left(\langle\hat{X}^2 + \hat{P}^2\rangle - 1\right) \tag{15}$$

$$\langle\hat{n}\rangle = \langle\hat{X}_\theta^2\rangle - \frac{1}{2}. \tag{16}$$

Thus calculating the expectation value of $\hat{X}_\theta^2$ gives us the mean number of photons. We can estimate $\langle\hat{n}\rangle$ by computing

$$\overline{\langle\hat{n}\rangle} = \frac{1}{N}\sum_{i=1}^{N} x_i^2 - \frac{1}{2}. \tag{17}$$

Note that when θ is uniformly distributed over $[0,\pi)$, the values of θ are not needed to compute $\overline{\langle\hat{n}\rangle}$.

Since we use known quantum states in our idealized numerical experiments, we can calculate the real mean number of photons in each state. This can be used to verify how good is the estimation using Eq. (17).

V. RESULTS

In study cases, we compute the fidelity between the true state and (i) the density matrix reconstructed without binning, ρ_{ML2}; (ii) the density matrix reconstructed using data binning with a random chosen bin width, ρ_{Hist}; (iii) and the density matrix reconstructed using data binning with a bin width given by Scott's method, ρ_{Scott}.

Our first result is shown in Fig. 1. The state considered is a cat state with amplitude $\alpha = 1$, and the Hilbert space was truncated at 10 photons. Scott method finds an optimal bin width for each phase considered, such that we have a mean bin width in this case. In here the mean bin width for Scott method is 0.35. When choosing a bin width, we go up to 0.34, the value we obtain when

we use Eq. (8) for $n = 10$, the number of photon for which we truncated the Hilbert space. In all cases, each bin's measurement operator represents a measurement that occurs at the center of the bin.

In Fig 1, each set of points corresponds to a different data set. Our goal was to check that different data sets would have similar behavior as we change the bin size. As we can see in this figure, the highest values of fidelity corresponds to the case where we do not apply any binning, as expected. We also see that the smaller the chosen bin width, the best are the results for the fidelity. However, the greatest loss in fidelity that we have is of 0.5%.

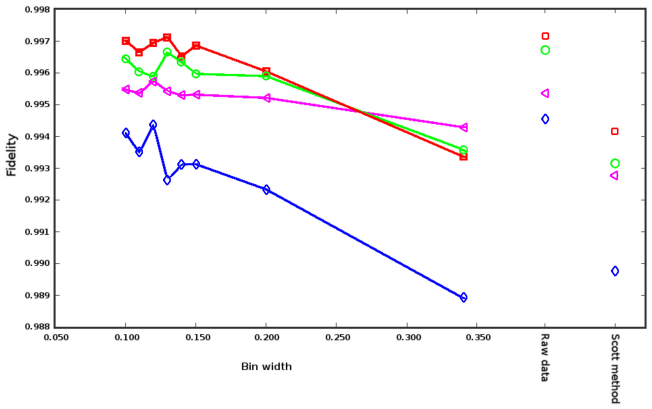

FIG. 1. Fidelity as a function of the bin width for a cat state with amplitude $\alpha = 1$. The Hilbert space is truncated at 10 photons. Each set of points corresponds to a different data set. The mean bin width for Scott method is 0.35.

The next set of results is presented in Fig. 2, where we have the fidelity as a function of the bin width for cat states with amplitudes $\alpha = 1$ and $\alpha = 2$. The states are reconstructed in a 15 photons Hilbert space. The first thing that we can notice in this graph is that the fidelity for a $\alpha = 1$ cat state is always greater than the fidelity for a $\alpha = 2$ cat state, including the case when we have no binning. This is expected, because a $\alpha = 2$ state requires more parameters to effectively describe its density matrix, so for a given amount of data, there is greater statistical uncertainty.

We may also notice that the fidelity for the $\alpha = 2$ cat state decreases faster than the fidelity for a $\alpha = 1$ cat state as the bin size increases. This is also expected because the $\alpha = 2$ state has more wiggles in its probability distribution, so more information is lost when the bins are larger. The average bin width for Scott method is 0.35 for a $\alpha = 1$ cat state, and 0.64 for a $\alpha = 2$ cat state.

Figure 3 shows the fidelity as a function of the bin width for a squeezed vacuum state whose squeezed quadrature has a variance 3/4 of the vacuum variance. We use a 15 photon Hilbert space to reconstruct this state. In this graph, we extended the bin width until 1.05 to help visualize the decreasing in the fidelity when the bin width increases. Using a bin width of 1.05 gives us a fidelity loss of about 7%, while the loss when we use

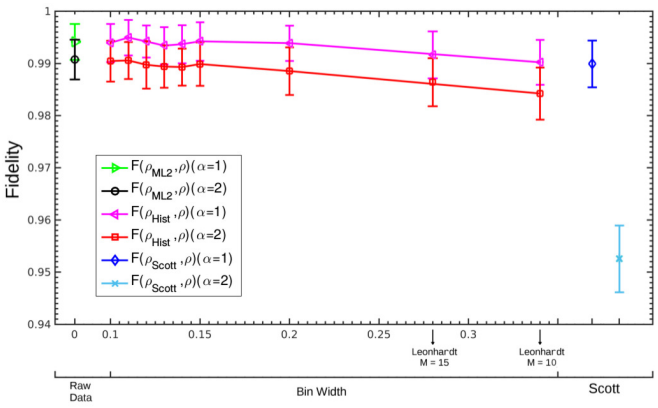

FIG. 2. Fidelity as a function of the bin width for cat states with amplitudes $\alpha = 1$ and $\alpha = 2$. The Hilbert space is truncated at 15 photons. The mean bin width for Scott method are 0.35 ($\alpha = 1$ cat state) and 0.64 ($\alpha = 2$ cat state).

Scott's optimal bin width (0.25) is of about 0.02%.

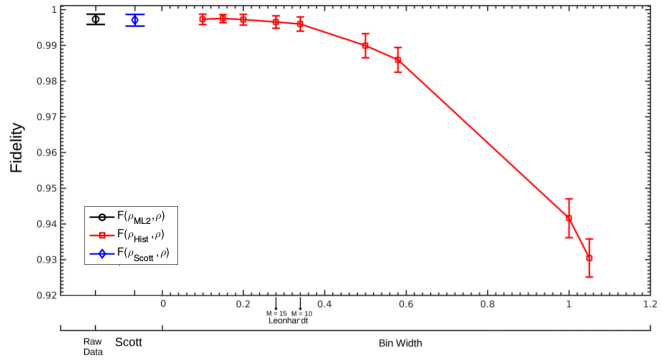

FIG. 3. Fidelity as a function of the bin width for a squeezed vacuum state whose squeezed quadrature has a variance 3/4 of the vacuum variance. The Hilbert space is truncated at 15 photons. The mean bin width for Scott method is 0.25.

Until now, as mentioned before, each bin's measurement operator represents a measurement that occurs at the center of the bin. In order to improve our analysis, we now change each bin's measurement operator so that it represents a measurement that occurs anywhere in the bin, rather than a measurement that happens exactly at the center of the bin. For that, we integrate the measurement operators over the width of each histogram bin. We will identify each case by adding [POVM-center] and [POVM-integral] to the fidelity identifier.

We also add to our analysis the fidelity calculation when using a bin width given by Leonhardt's formula, Eq. (8), calculated with the mean photon number estimated by Eq. (17). In this case, we compute the fidelity between the true state and the density matrix reconstructed using data binning with a bin width given by Leonhardt formula, $\rho_{\text{Leonhardt}}$. We reminder the reader

that Leonhardt suggests that the used bin width should be equal or smaller to the one calculated using Eq. (8).

In Figs. 4 and 5, we have the fidelity as a function of the bin width for cat states with amplitudes $\alpha = 1$ and $\alpha = 2$, respectively. We used a 10 photon Hilbert space to reconstruct the $\alpha = 1$ cat state, while the $\alpha = 2$ cat state was reconstructed in a 15 photon space. On the other hand, Fig. 6 shows the fidelity as a function of the bin width for a squeezed vacuum state whose squeezed quadrature has a variance 3/4 of the vacuum variance, with a Hilbert space truncated at 10 photons.

For the $\alpha = 1$ cat state in Fig. 4, the estimated mean number of photons is 0.6109 (real mean number of photons is 0.6093), what gives us, by Leonhardt's formula, Eq. (8), a bin width of 1.05. As mentioned before, the average bin width for Scott method in this case is 0.35. For the $\alpha = 2$ cat state in Fig. 5, the estimated mean number of photons is 3.1983 (real mean number of photons is 3.1978), giving a bin width of 0.58. The average bin width for Scott method is 0.64 for this state. The squeezed vacuum state of Fig. 6 has an estimated mean number of photons of 0.0162 (real mean number of photons is 0.0167), giving a bin width, by Eq. (8), of 1.54. The average bin width for Scott method, in this case, is 0.25.

Analyzing the graphs shown in Figs. 4-6, we see that integrating the measurement operators over the width of each histogram bin improves considerably the fidelity for all the cases. We can also see that, for this case, Leonhardt's suggestion can be safely considered an upper bound for the bin width. The two methods considered here, Leonhardt and Scott methods, give faster fidelity estimates with no significant loss of information.

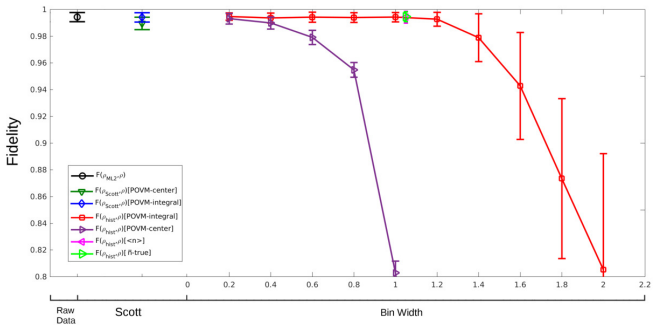

FIG. 4. Fidelity as a function of the bin width for a cat state with amplitude $\alpha = 1$. The Hilbert space is truncated at 10 photons. The mean bin width for Scott method is 0.35, and the bin width given by Leonhardt formula is 1.05.

VI. CONCLUSION

We have used idealized numerical experiments to generate simulated data, performed tomography on the data with and without binning, and estimated the fidelity between the reconstructed state and the true state. We

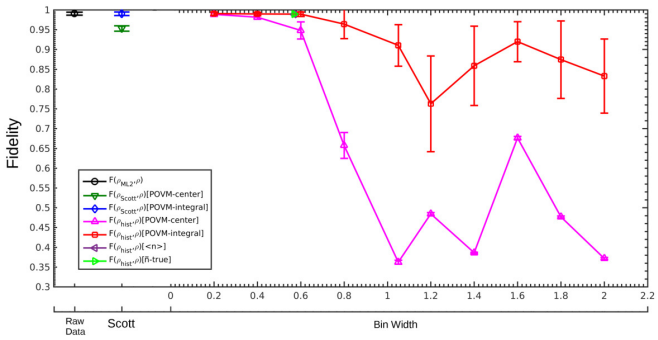

FIG. 5. Fidelity as a function of the bin width for a cat state with amplitude $\alpha = 2$. The Hilbert space is truncated at 15 photons. The mean bin width for Scott method is 0.64, and the bin width given by Leonhardt formula is 0.58.

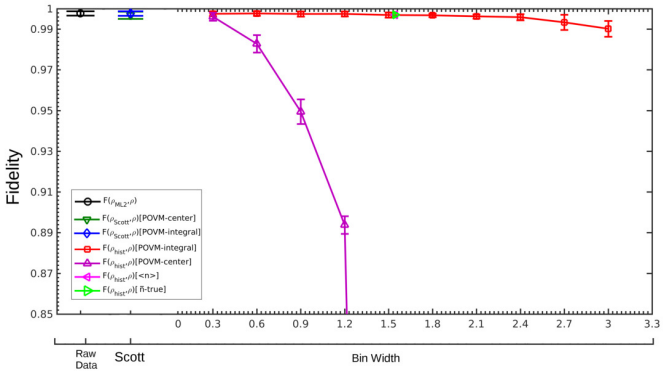

FIG. 6. Fidelity as a function of the bin width for a squeezed vacuum state whose squeezed quadrature has a variance 3/4 of the vacuum variance. The Hilbert space is truncated at 10 photons. The mean bin width for Scott method is 0.25, and the bin width given by Leonhardt formula is 1.54.

used two different methods to choose the bin width: Scott and Leonhardt methods. We considered the bins measurement operator to represent a measurement that occurs at the center of the bin or anywhere in the bin. Our study has focused on maximum likelihood tomography of cat states and squeezed vacuum states.

Scott method calculates an optimal bin width, for each phase, based on the size and the standard deviation of the sample. Leonhardt states that we need a bin width narrower than $q_n/2$, where q_n depends on the number of photons in the state being reconstructed. Since, in a real experiment, we may not know the mean number of photons in the state considered, we have proposed a method to determine the mean photon number from the quadrature measurement results.

We have found that our proposed method to find the mean number of photons from the quadrature measurement results gives accurate results. We checked that by comparing the estimated mean number of photons with the real mean number of photons for the known states we considered: cat states and squeezed vacuum states. We

also have found that integrating the measurement operators over the width of each histogram bin improves significantly the fidelity. Using this strategy, Leonhardt formula safely establishes an upper bound to the bin width, and both methods provides a faster statistical estimation without losing too much information.

ACKNOWLEDGMENTS

We thank Kevin Coakley, Adam Keith, and Emanuel Knill for helpful comments on the manuscript. H. M. Vasconcelos thanks the Schlumberger Foundation's Faculty for the Future program for financial support. J. L. E. Silva thanks Coordenação de Aperfeiçoamento de Pessoal de Nível Superior (CAPES) for financial support. This work includes contributions of the National Institute of Standards and Technology, which are not subject to U.S. copyright.

[1] A. Kandala, A. Mezzacapo, K. Temme, M. Takita, M. Brink, J. M. Chow, and J. M. Gambetta, "Hardware-efficient quantum optimizer for small molecules and quantum magnets," Nature **549**, 242–246 (2014), arXiv:arXiv:1704.05018.

[2] N. M. Linke, D. Maslov, M. Roetteler, S. Debnath, C. Figgatt, K. A. Landsman, K. Wright, and C. Monroe, "Experimental comparison of two quantum computing architectures," Proc. Natl. Acad. Sci. U. S. A. **114**, 3305–3310 (2017).

[3] T. Monz, D. Nigg, E. A. Martinez, M. F. Brandl, P. Schindler, R. Rines, S. X. Wang, I. L. Chuang, and R. Blatt, "Realization of a scalable shor algorithm," Science **351**, 1068–1070 (2017).

[4] V. S. Denchev, S. Boixo, S. V. Isakov, N. Ding, R. Babbush, V. Smelyanskiy, J. Martinis, and H. Neven, "What is the computational value of finite-range tunneling?" Phys. Rev. X **6**, 031015 (2016).

[5] K. Vogel and H. Risken, "Determination of quasiprobability distributions in terms of probability distributions for the rotated quadrature phase," Phys. Rev. A **40**, 2847–2849 (1989).

[6] D. T. Smithey, M. Beck, M. G. Raymer, and A. Faridani, "Measurement of the wigner distribution and the density matrix of a light mode using optical homodyne tomography: Application to squeezed states and the vacuum," Phys. Rev. Lett. **70**, 1244–1247 (1993).

[7] T. Dunn, I. A. Walmsley, and S. Mukamel, "Experimental determination of the quantum-mechanical state of a molecular vibrational mode using fluorescence tomography," Phys. Rev. Lett. **74**, 884–887 (1995).

[8] K. Banaszek, C. Radzewicz, K. Wodkiewicz, and J. S. Krasinski, "Direct measurement of the wigner function by photon counting," Phys. Rev. A **60**, 674–677 (1999).

[9] K. Banaszek, G. M. D'Ariano, M. G. A. Paris, and M. F. Sacchi, "Maximum-likelihood estimation of the density matrix," Phys. Rev. A **61**, 010304(R) (2000).

[10] A. G. White, D. F. V. James, W. J. Munro, and P. G. Kwiat, "Exploring hilbert space: Accurate characterization of quantum information," Phys. Rev. A **65**, 012301 (2002).

[11] A. Ourjoumtsev, H. Jeong, R. Tualle-Brouri, and P. Grangier, "Generation of optical 'schrödinger cats' from photon number states," Nature **448**, 784–786 (2007).

[12] J. S. Neergaard-Nielsen, B. Melholt Nielsen, C. Hettich, K. Mø lmer, and E. S. Polzik, "Generation of a superposition of odd photon number states for quantum information networks," Phys. Rev. Lett..

[13] I. L. Chuang and M. A. Nielsen, "Prescription for experimental determination of the dynamics of a quantum black box," J. Mod. Optics **44**, 2455–2467 (1997).

[14] J. F. Poyatos, J. I. Cirac, and P. Zoller, "omplete characterization of a quantum process: The two-bit quantum gate," Phys. Rev. Lett. **78**, 390–393 (1997).

[15] J. B. Altepeter, D. Branning, E. Jeffrey, T. C. Wei, P. G. Kwiat, R. T. Thew, J. L. OBrien, M. A. Nielsen, and A. G. White, "Ancilla-assisted quantum process tomography," Phys. Rev. Lett. **90**, 193601 (2003).

[16] G. M. D'Ariano and L. Maccone, "Measuring quantum optical hamiltonians," Phys. Rev. Lett. **80**, 5465–5468 (1998).

[17] M. A. Nielsen, E. Knill, and R. Laflamme, "Complete quantum teleportation using nuclear magnetic resonance," Nature.

[18] M. W. Mitchell, C. W. Ellenor, S. Schneider, and A. M. Steinberg, "Diagnosis, prescription and prognosis of a bell-state filter by quantum process tomography," Phys. Rev. Lett..

[19] J. L. O'Brien, G. J. Pryde, A. Gilchrist, D. F. V. James, N. K. Langford, T. C. Ralph, and A. G. White, "Quantum process tomography of a controlled-not gate," Phys. Rev. Lett..

[20] C. Kupchak, S. Rind, B. Jordaan, and E. Figueroa, "Quantum process tomography of an optically-controlled kerr non-linearity," Sci. Rep. **5**, 16581 (2015).

[21] A. Luis and L. L. Sanchez-Soto, "Complete characterization of arbitrary quantum measurement processes," Phys. Rev. Lett. **83**, 3573–3576 (1999).

[22] J. Fiurasek, "Maximum-likelihood estimation of quantum measurement," Phys. Rev. A **64**, 024102 (2001).

[23] G. M. D'Ariano, L. Maccone, and P. Lo Presti, "Quantum calibration of measurement instrumentation," Phys. Rev. Lett. **93**, 250407 (2004).

[24] J. S. Lundeen, A. Feito, H. Coldenstrodt-Ronge, K. L. Pregnell, Ch. Silberhorn, T. C. Ralph, J. Eisert, M. B. Plenio, and I. A. Walmsley, "Tomography of quantum detectors," Sci. Rep. **5**, 27–30 (2009).

[25] S. Lloyd and S. L. Braunstein, "Quantum computation over continuous variables," Phys. Rev. Lett. **82**, 1784 (1999).

[26] D. Gottesman, A. Kitaev, and J. Preskill, "Encoding a

qubit in an oscillator," Phys. Rev. A **64**, 012310 (2001).
[27] S. D. Bartlett, H. de Guise, and B. C. Sanders, "Quantum encodings in spin systems and harmonic oscillators," Phys. Rev. A **65**, 052316 (2002).
[28] H. Jeong and M. S. Kim, "Efficient quantum computation using coherent states," Phys. Rev. A **65**, 042306 (2002).
[29] T. Ralph, A. Gilchrist, G. Milburn, W. Munro, and S. Glancy, "Quantum computation with optical coherent state," Phys. Rev. A **68**, 042319 (2003), quant-ph/0306004.
[30] T. Ralph, "Continuous variable quantum cryptography," Phys. Rev. A **61**, 010303(R) (1999).
[31] M. Hillery, "Quantum cryptography with squeezed states," Phys. Rev. A **61**, 022309 (2000).
[32] Ch. Silberhorn, T. C. Ralph, N. Lü tkenhaus, and G. Leuchs, "Continuous variable quantum cryptography: Beating the 3 db loss limit," Phys. Rev. Lett. **89**, 167901 (2002).
[33] S. Pirandola, S. Mancini, S. Lloyd, and S. L. Braunstein, "Continuous-variable quantum cryptography using two-way quantum communication," Nature Phys. **4**, 726–730 (2008), arXiv:quant-ph/0304059.
[34] F. S. Luiz and G. Rigolin, "Teleportation-based continuous variable quantum cryptography," **16**, 58 (2017).
[35] T. Eberle, S. Steinlechner, J. Bauchrowitz, V. Hä ndchen, H. Vahlbruch, M. Mehmet, H. Mü ller Ebhardt, , and R. Schnabel, "Quantum enhancement of the zero-area sagnac interferometer topology for gravitational wave detection," Phys. Rev. Lett. **104**, 251102 (2004).
[36] R. Demkowicz-Dobrzaski, K. Banaszek, and R. Schnabel, "Fundamental quantum interferometry bound for the squeezed-light-enhanced gravitational wave detector geo 600," Phys. Rev. A **88** (2013).
[37] L. Vaidman, "Teleportation of quantum states," Phys. Rev. A **49**, 1473 (1994).
[38] S. L. Braunstein and H. J. Kimble, "Teleportation of continuous quantum variables," Phys. Rev. Lett. **80**, 869 (1998).
[39] Q. He, L. Rosales-Zrate, G. Adesso, and M. D. Reid, "Secure continuous variable teleportation and einstein-podolsky-rosen steering," Phys. Rev. Lett. **115**, 180502 (2015).
[40] S. L. Braunstein and H. J. Kimble, "Dense coding for continuous variables," Phys. Rev. A **61**, 042302 (2000).
[41] J. Lee, S. Ji, J. Park, and H. Nha, "Continuous-variable dense coding via a general gaussian state: Monogamy relation," Phys. Rev. A **90**, 022301 (2014).
[42] N. J. Cerf and S. Iblisdir, "Optimal n-to-m cloning of conjugate quantum variables," Phys. Rev. A **62**, 040301(R) (2000).
[43] S. L. Braunstein, N. J. Cerf, S. Iblisdir, P. van Loock, and S. Massar, "Optimal cloning of coherent states with a linear amplifier and beam splitters," Phys. Rev. Lett. **86**, 4938 (2001).
[44] D. Scott, "Scott's rule," WIREs Comp. Stat. **2**, 497–502 (2010).
[45] U. Leonhardt, Measuring the Quantum State of Light (Cambridge University Press, New York, 1997).
[46] Jaroslav Řeháček, Zdeněk Hradil, E. Knill, and A. I. Lvovsky, "Diluted maximum-likelihood algorithm for quantum tomography," Phys. Rev. A **75**, 042108 (2007), arXiv:quant-ph/0611244v2.
[47] S. C. Glancy, E. Knill, and M. Girard, "Gradient-based stopping rules for maximum-likelihood quantum-state tomography," New J. Phys. **14**, 095017 (2012), arXiv:1205.4043 [quant-ph].
[48] A. I. Lvovsky and M. G. Raymer, "Continuous-variable optical quantum-state tomography," Rev. Mod. Phys. **81**, 299 (2009), arXiv:quant-ph/0511044.
[49] William J. Kennedy Jr. and James E. Gentle, Statistical Computing (Marcel Dekker, Inc., New York, 1980) see section 6.4.3.
[50] U. Leonhardt, M. Munroe, T. Kiss, Th. Richter, and M.G. Raymer, "Sampling of photon statistics and density matrix using homodyne detection," Opt. Commun. **127**, 144–160 (1996).
[51] C. Schwemmer, L. Knips, D. Richart, H. Weinfurter, T. Moroder, M. Kleinmann, and O. Gühne, "Systematic errors in current quantum state tomography tools," Phys. Rev. Lett. **114**, 080403 (2015), arXiv:1310.8465 [quant-ph].
[52] B. Efron and R. J. Tibshirani, An Introduction to the Bootstrap (Chapman and Hall, New York, 1993).
[53] R. Blume-Kohout, "Robust error bars for quantum tomography," (2012), arXiv:1202.5270 [quant-ph].
[54] M. Christandl and R. Renner, "Reliable quantum state tomography," Phys. Rev. Lett. **109**, 120403 (2012), arXiv:1108.5329v1.
[55] Philippe Faist and Renato Renner, "Practical and reliable error bars in quantum tomography," Phys. Rev. Lett. **117**, 010404 (2016), arXiv:1509.06763 [quant-ph].